

## Piezoelectric Behavior in Bio-Derived Prawn and Crab Shells: A Comparative Analysis

Ramar Marimuthu<sup>\*1</sup>, Santhosh Kumar Pandidurai<sup>1</sup>, Rathipriya Mahadevan<sup>1</sup>, Kesavan Devarayan<sup>1</sup>,  
Palani Rasu<sup>2</sup>, Monikandon Sukumaran<sup>1</sup>

<sup>1</sup>College of Fisheries Engineering, Tamil Nadu Dr. J. Jayalalithaa Fisheries University, Nagapattinam - 611 002, Tamil Nadu, India

<sup>2</sup>Dr.M.G.R. Fisheries College and Research Institute, Tamil Nadu Dr. J. Jayalalithaa Fisheries University, Thalainayeru, Nagapattinam - 614 712, Tamil Nadu, India

### Abstract

Piezoelectric films were fabricated from biowaste derived from prawn shells (PS) and crab shells (CS). UV–Vis spectroscopy revealed distinct absorption peaks at 266 nm and 377 nm for processed PS, and at 249 nm and 276 nm for processed CS. In the visible spectral range, the transmittance of PS and CS films was measured at approximately 40%–46% and 40%–43%, respectively. Structural and crystallographic characteristics were examined using Fourier Transform Infrared Spectroscopy (FTIR), confirming the presence of both intra- and intermolecular hydrogen bonding, as evidenced by vibrational bands at 3145  $\text{cm}^{-1}$  and 3011  $\text{cm}^{-1}$  for PS, and 3328  $\text{cm}^{-1}$  and 3159  $\text{cm}^{-1}$  for CS. Raman spectroscopy further verified the presence of amino acids within the triple-helical structure of polypeptide chains in both PS and CS. The inherent flexibility and piezoelectric properties of these bio-derived films highlight their potential for use in energy-harvesting device applications.

**Keywords:** bio waste, prawn shell, crab shell, piezoelectric, flexibility, energy harvesting

### \*Correspondence

Author: Ramar Marimuthu  
Email: ramar@tnfu.ac.in

### Introduction

Piezoelectric materials possess the unique ability to generate electrical charges in response to applied mechanical stress. Rochelle salt, the first identified piezoelectric material, was initially developed for medical applications [1–4]. The piezoelectric effect was first discovered by the Curie brothers, who observed the phenomenon while studying crystalline solids such as quartz, cane sugar, and Rochelle salt. Their findings established that piezoelectricity is intrinsically linked to the asymmetry of crystal structures [5, 6]. A major milestone in the evolution of piezoelectric materials was the discovery of significant piezoelectric coefficients in synthetic polymers, particularly polyvinylidene fluoride (PVDF), which opened new avenues for flexible and lightweight piezoelectric devices. PVDF is widely employed in sensing and energy harvesting applications due to its unique intrinsic properties, including a high surface area, elevated surface-to-volume ratio, and superior electrical, chemical, and optical characteristics. As a semi-crystalline polymer, PVDF can crystallize into four distinct phases:  $\alpha$ ,  $\beta$ ,  $\gamma$ , and  $\delta$ . The  $\alpha$ -phase, which is nonpolar, is most commonly observed in polymer solutions. In contrast, the  $\beta$ -phase exhibits aligned molecular dipoles, resulting in strong polarization characteristics. This phase is particularly notable for its exceptional ferroelectric and piezoelectric behavior, leading to the highest spontaneous polarization among all PVDF phases [7–12].

The crab exoskeleton is a hierarchical three-dimensional biocomposite, consisting of brittle chitin–protein fibrils arranged in a Bouligand (twisted plywood) pattern within the x–y plane, and ductile pore canal tubules oriented perpendicularly to the surface (z-direction). Remarkably, these pore canal tubules retain their ductile mechanical behavior even in the dehydrated state. The endocuticle displays a highly porous architecture, with individual lamellae measuring approximately 10–15  $\mu\text{m}$  in thickness. This region exhibits relatively low stiffness, with elastic moduli of 471 MPa in the claw and 142 MPa in the walking leg segments. According to Po-Yu Chen (2008), the experimentally observed compressive strength of the crab exoskeleton (57 MPa) slightly exceeds the predicted value of 50 MPa [13–18]. In parallel, the improper disposal of prawn shell waste (PSW), a byproduct of the fisheries and aquaculture industries, has become a pressing environmental issue due to the accumulation of non-biodegradable marine biomass [19].

The shellfish industry is active across all coastal countries, generating significant amounts of waste during processing. Typically, the edible flesh of prawns and crabs is separated, while the heads and shells are discarded, resulting in the release of substantial organic waste worldwide. It is estimated that the industry produces between 60,000 and 80,000 tonnes of shell waste annually [20-22]. Although these wastes are biodegradable, their decomposition is slow due to the large volumes generated during each processing cycle [23-25]. Over time, this accumulation causes environmental problems by emitting unpleasant odors and attracting disease vectors such as flies, rats, and other pests, thereby creating unsanitary conditions. An urgent and sustainable solution is the prompt recycling of crustacean shells and the recovery of valuable bioactive compounds for various industrial applications [26, 27].

Piezoelectric power generation encompasses a broad spectrum of applications in electricity production and offers significant socio-economic benefits throughout the industrial value chain from the manufacturing of electrical components to energy harvesting. This study aims to critically assess the feasibility of piezoelectric power generation systems by examining fundamental operating principles and exploring potential system configurations. The insights gained will provide a robust foundation for advancing future research and innovation in this promising technology. This paper presents the development of piezoelectric films fabricated from PS and CS biowaste, marking a notable advancement in the field of biodegradable piezoelectric materials. Comprehensive molecular characterization was performed using UV-visible spectroscopy and spectrophotometry, complemented by detailed analyses of structural and chemical features through FTIR and Raman spectroscopy. The primary aim of this study is to investigate these novel biodegradable piezoelectric biomaterials, deepen understanding of the mechanisms underlying their piezoelectricity, and explore their potential for innovative applications in wearable and implantable bioelectronic devices.

## Materials and Methods

The raw fresh specimens of *Penaeus monodon* (giant tiger prawn) and *Portunus sanguinolentus* (three-spotted crab) were collected from the Akkaraipet Fish Landing Center, Nagapattinam, Tamil Nadu. The prawn and crab shells were subjected to demineralization and deproteinization processes using the following reagents: sodium hydroxide (NaOH), sodium chloride (NaCl), tris (hydroxymethyl) amino methane hydrochloride (Tris-HCl), and ethylene diamine tetra acetic acid (EDTA).

### **Sample Preparation**

#### *Shell Collection and Cleaning*

Fresh prawns (*Penaeus monodon*) and crabs (*Portunus sanguinolentus*) were peeled, and their shells thoroughly washed with double-distilled water to remove impurities and residues.

#### *Demineralization Process*

The cleaned shells were subjected to demineralization by immersing them in a solvent mixture containing 0.5 M NaOH, 1.0 M NaCl, 0.05 M (Tris-HCl), and 20.0 mM EDTA. The samples were agitated at 180–190 rpm using a Spimax orbital shaker. The EDTA solution was prepared separately with a magnetic stirrer to ensure complete dissolution.

#### *EDTA Soaking*

Following initial treatment, the shells were further soaked in a 0.5 M EDTA solution to enhance demineralization, resulting in more translucent and flexible materials suitable for piezoelectric applications.

#### *Drying*

After immersion, shells were air-dried at room temperature for several minutes before being transferred to vacuum desiccators for thorough drying. Post-demineralization, the shells displayed increased transparency and pliability.

#### *Electrical Contact Preparation*

To enable electrical measurements, the dried shells were coated with copper tape strips. These copper-coated shells were then soldered using lead-based solder to attach conducting wires, facilitating the extraction of electrical energy generated from the piezoelectric effect.

## Results and Discussion

**Figure 1** illustrates the UV–Visible absorption spectra of the treated prawn and crab shells. UV–Visible spectroscopy was utilized to evaluate the structural integrity and quality of collagen nanofibrils within the demineralized shells over the 200–800 nm wavelength range. The piezoelectric films derived from prawn shells displayed distinct absorption maxima at 266 nm and 377 nm, whereas those from crab shells exhibited prominent peaks at 249 nm and 276 nm. These characteristic absorption features reflect differences in molecular composition and structural organization between the two biowaste-derived films.

**Figure 2** represents the FT-IR spectra of the processed prawn and crab shells. The spectra clearly demonstrate the presence of both intra- and intermolecular hydrogen bonding within the prawn shell, as evidenced by the characteristic vibrational bands at  $3145\text{ cm}^{-1}$  and  $3011\text{ cm}^{-1}$ . Moreover, the amide I band exhibits a distinct splitting into two peaks at  $1660\text{ cm}^{-1}$  and  $1589\text{ cm}^{-1}$ , corresponding to intramolecular hydrogen bonds and intersheet C=O–NH hydrogen bonds, respectively. The absorption peak at  $1417\text{ cm}^{-1}$  is attributed to the amide II band, further confirming the complex hydrogen bonding network within the biomaterial.

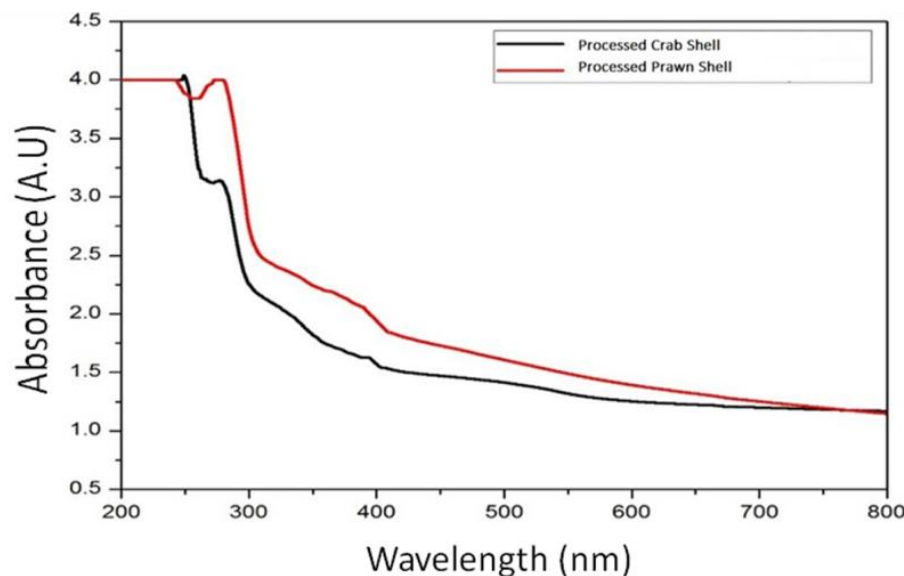


**Figure 1** UV-visible absorption characteristics of processed prawn and crab shell films

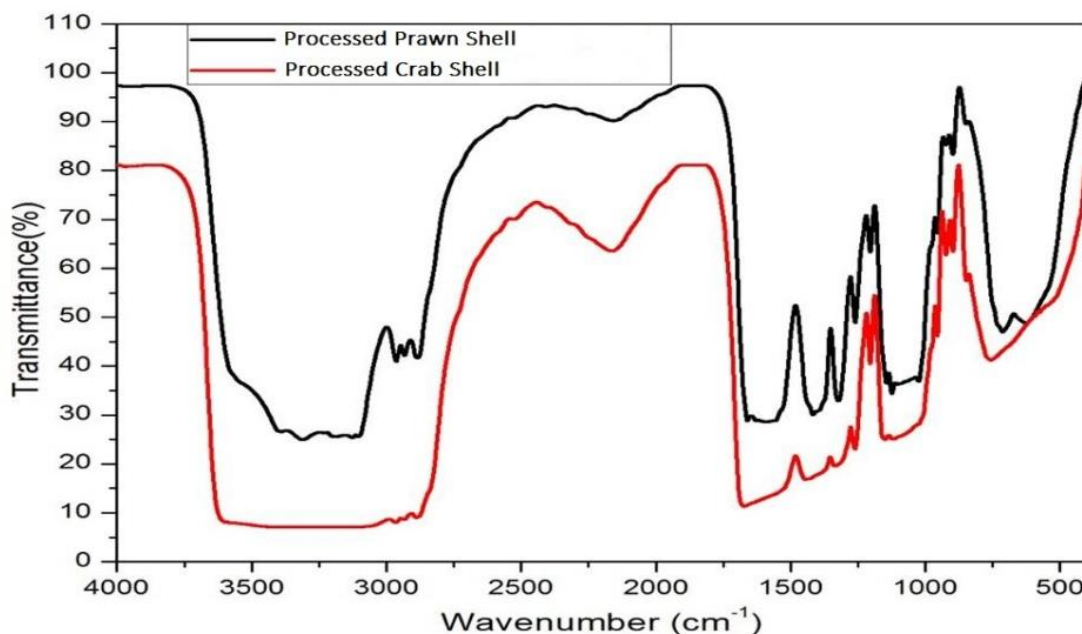


**Figure 2** Fourier Transform Infrared (FT-IR) spectra illustrating the key functional groups and bonding characteristics in processed prawn and crab shells

The vibrational bands at  $3328\text{ cm}^{-1}$  and  $3159\text{ cm}^{-1}$  in the crab shell spectrum indicate the coexistence of intra- and intermolecular hydrogen bonds. The amide I band exhibits a clear splitting into two peaks at  $1673\text{ cm}^{-1}$  and  $1447\text{ cm}^{-1}$ , reflecting the presence of intramolecular hydrogen bonds and intersheet C=O-NH hydrogen bonding, respectively. Additionally, the absorption peak at  $1337\text{ cm}^{-1}$  is characteristic of the amide II band, further substantiating the complex hydrogen bonding network within the crab shell matrix.

Raman spectroscopy confirms the presence of amino acids within the triple helix structure of polypeptide chains in both raw and processed prawn shells (Figure 3). The prominent band at  $1656\text{ cm}^{-1}$  in the processed prawn shell is attributed to the stretching vibration of the carbonyl group (C=O) in the peptide backbone of the Gly-X-Y tripeptide sequence, corresponding to the amide I band. A strong absorbance at  $1448\text{ cm}^{-1}$  arises from  $\text{CH}_2$  deformation ( $\delta(\text{CH}_2)$ ). Vibrational bands at  $1259\text{ cm}^{-1}$  and  $1250\text{ cm}^{-1}$  are assigned to in-plane N-H bending ( $\delta(\text{N}-\text{H})$ ) coupled with C-N stretching ( $\nu(\text{C}-\text{N})$ ), characteristic of the amide III band, which signifies the polar triple helix conformation of collagen.

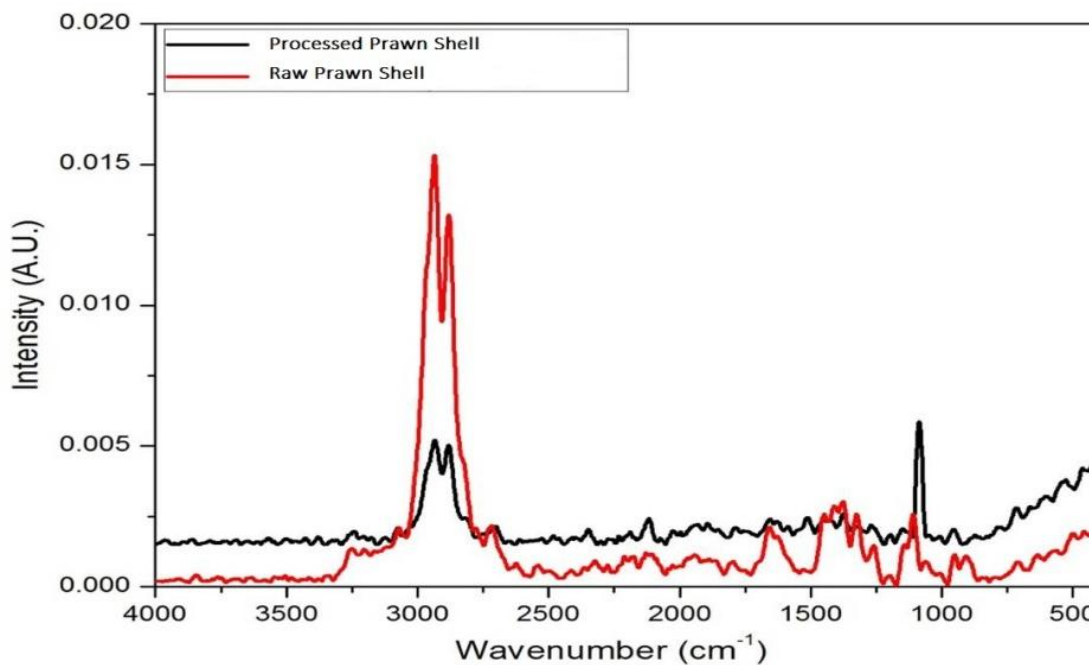


**Figure 3** Raman spectra illustrating the molecular and structural characteristics of processed prawn shell.

Additional bands associated with carboxyl groups appear at  $1377\text{ cm}^{-1}$  (aspartic acid) and  $1040\text{ cm}^{-1}$  (glutamic acid), while protonated amino groups such as  $\text{NH}_3^+$  are observed at  $1110\text{ cm}^{-1}$ . Amino acids including phenylalanine ( $1047\text{ cm}^{-1}$  and  $955\text{ cm}^{-1}$ ), proline ( $908\text{ cm}^{-1}$  and  $870\text{ cm}^{-1}$ ), and hydroxyproline ( $885\text{ cm}^{-1}$ ) show significant Raman scattering due to their aromatic or cyclic side chains within the  $1000$ – $800\text{ cm}^{-1}$  spectral region. The peak at  $950\text{ cm}^{-1}$  corresponds to C-C stretching vibrations of the peptide backbone.

Collectively, these spectral features validate the integrity of the helical collagen structure in prawn shells, specifically highlighting the Gly-Pro-Y and Gly-X-Hyp tripeptide motifs. This well-preserved triple helix structure is crucial for the piezoelectric response, as the ordered arrangement of polar peptide bonds facilitates the generation of electrical charges under mechanical stress.

Raman spectroscopy confirms the presence of amino acids within the triple helix structure of polypeptide chains in the crab shell (Figure 4). The band at  $1621\text{ cm}^{-1}$  in the processed crab shell is attributed to the stretching vibration ( $\nu$ ) of the carbonyl group (C=O) in the peptide backbone of the Gly-X-Y tripeptide sequence, corresponding to the amide I band. A pronounced absorbance at  $1410\text{ cm}^{-1}$  arises from  $\text{CH}_2$  deformation ( $\delta(\text{CH}_2)$ ). The amide III band is characterized by vibrational peaks at  $1267\text{ cm}^{-1}$  and  $1248\text{ cm}^{-1}$ , which result from in-plane N-H bending ( $\delta(\text{N}-\text{H})$ ) coupled with C-N stretching ( $\nu(\text{C}-\text{N})$ ), indicative of the polar triple helix conformation of collagen.

Additional bands associated with carboxyl groups appear at  $1410\text{ cm}^{-1}$  (aspartic acid) and  $1060\text{ cm}^{-1}$  (glutamic acid), while protonated amino groups such as  $\text{NH}_3^+$  are detected at  $1110\text{ cm}^{-1}$ . Amino acids including phenylalanine ( $1060\text{ cm}^{-1}$  and  $955\text{ cm}^{-1}$ ), proline ( $915\text{ cm}^{-1}$  and  $865\text{ cm}^{-1}$ ), and hydroxyproline ( $880\text{ cm}^{-1}$ ) display significant Raman scattering due to their aromatic or cyclic side chains within the  $1060$ – $930\text{ cm}^{-1}$  spectral range. The peak at  $955\text{ cm}^{-1}$  corresponds to C-C stretching vibrations of the peptide backbone.

Collectively, these spectral features confirm the structural integrity of the helical collagen in crab shells, specifically emphasizing the Gly-Pro-Y and Gly-X-Hyp tripeptide motifs fundamental to its biological function and mechanical

properties. The ordered arrangement of these polar peptide bonds within the triple helix is essential for the crab shell's piezoelectric response, enabling efficient conversion of mechanical stress into electrical signals.

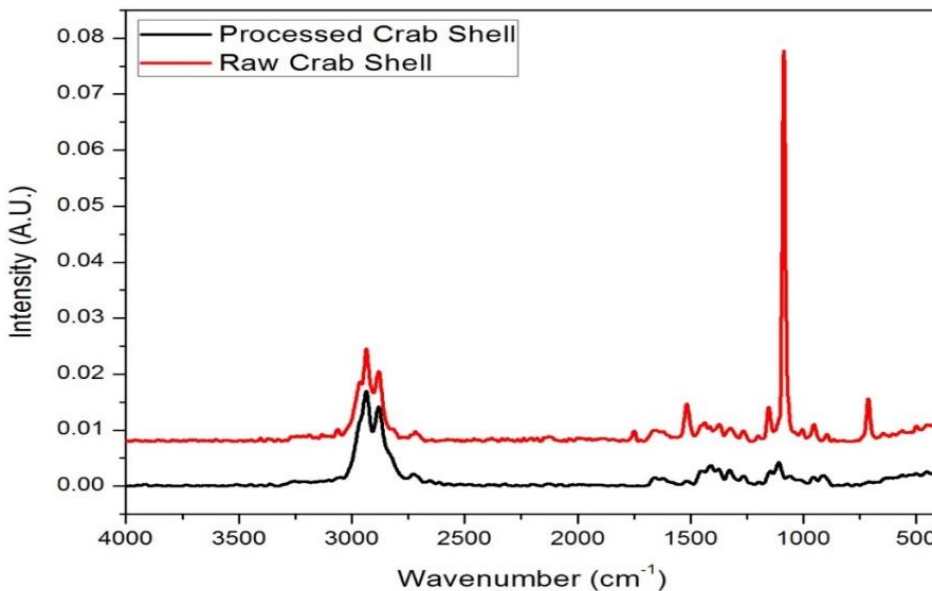


**Figure 4.** Raman spectra illustrating the molecular and structural characteristics of processed crab shell.

## Conclusion

This study successfully developed and characterized piezoelectric films from PS and CS bio-waste. The processed prawn shell exhibited distinct UV absorption peaks at 266 nm and 377 nm, whereas the crab shell showed peaks at 249 nm and 276 nm. Both materials demonstrated comparable visible light transmittance, with PS ranging from 40% to 46% and CS from 40% to 43%. Structural and crystallographic analyses via FTIR revealed characteristic molecular features, while Raman spectroscopy confirmed the preservation of collagen's triple helix structure, underpinning the films' piezoelectric behavior. The inherent flexibility of these bio-derived films, combined with their piezoelectric properties, makes them promising candidates for sustainable energy harvesting applications. Furthermore, utilizing seafood waste not only addresses environmental concerns related to shellfish byproducts but also presents an eco-friendly approach with significant commercialization potential in wearable and implantable bioelectronics.

## Acknowledgement

The authors sincerely acknowledge the Tamil Nadu Dr. J. Jayalalithaa Fisheries University, Nagapattinam, Tamil Nadu, India, for the generous financial support provided under the Junior Teacher's Research Fellowship (JTRF) Scheme (U.S.O. No. 1106/B3/JTRF/2021, RC No. 5537/B3/JTRF/2021, SI No. 3). This research is also partially funded by Unnat Bharat Abhiyan 2.0 (UBA 2.0) Project No: RP-03525G. The authors also appreciate the continuous encouragement and support extended by the university throughout the course of this research.

## References

- [1] G. Busch. Early history of ferroelectricity. *Ferroelectrics*, 1987, 74:267-284
- [2] J. Valasek. Piezo-electric and allied phenomena in Rochelle salt. *Physical Review*, 1921, 17:475-481.
- [3] M. Ramar, S. Balasubramanian. Development of Piezoelectric Property Materials for the Nanogenerator Production. *Research Journal of Chemical and Environmental Sciences*, 2018, 6:114-123.
- [4] I. Kierzewski, S.S. Bedair, B. Hanrahan, H. Tsang, L. Hu, N. Lazarus. Adding an electroactive response to 3D printed materials: Printing a piezoelectret. *Additive Manufacturing*, 2020, 31:100963.
- [5] W. P. Mason. Piezoelectricity, Its history and applications. *The Journal of the Acoustical Society of America*, 1981, 70:1561-1566.
- [6] R. Marimuthu, K. Devarayan, M. Sukumaran, P. Rasu, L. Maruthu, M. Ramasamy, S. Muruganantham. Eco-friendly piezoelectric energy harvester from crustacean shells. *AIP Conference Proceedings*, 2024, 3122( 1): 050016-1-050016-5.
- [7] R. Kepler. Ferroelectricity in polyvinylidene fluoride. *Journal of Applied Physics*, 1978, 49:1232-1235.

[8] H. Kawai. The Piezoelectricity of Poly (vinylidene Fluoride). *Japanese Journal of Applied Physics*, 1969, 8:975-976.

[9] D. Bokov, A. Turki Jalil, S. Chupradit, W. Suksatan, M. Javed Ansari, I.H. Shewael, G.H. Valiev, E. Kianfar. Nanomaterial by sol-gel method: synthesis and application. *Advances in Materials Science and Engineering*, 2021, 2021: 5102014-1-5102014-21.

[10] M. Patel, S. Mishra, R. Verma, D. Shikha. Synthesis of ZnO and CuO nanoparticles via sol gel method and its characterization by using various technique. *Discover Materials*, 2022, 2:1.

[11] L. Mi, Q. Zhang, H. Wang, Z. Wu, Y. Guo, Y. Li, X. Xiong, K. Liu, W. Fu, Y. Ma, B. Wang, X. Qi. Synthesis of BaTiO<sub>3</sub> nanoparticles by sol-gel assisted solid phase method and its formation mechanism and photocatalytic activity. *Ceramics International*, 2020, 46:10619–10633.

[12] S. Sharma, M. Hasan, K.V. Rajulapati, R. Kumar, P.M. Ajayan, R.M. Yadav. Investigations on dielectric and mechanical properties of poly(vinylidene fluoride- hexafluoropropylene) (PVDF-HFP)/single-walled carbon nanotube composites. *Journal of Nanoparticle Research*, 2023, 25:246 (1-14).

[13] Kishore Kumar Gadgey, Amit Bahekar. Investigation of mechanical properties of crab shell: a review. *International Journal of Latest Trends in Engineering and Technology*, 2017, 8(1):268-281.

[14] T. Zhang, K. Xu, J. Li, L. He, D. W. Fu, Q. Ye, R. G. Xiong. Ferroelectric hybrid organic-inorganic perovskites and their structural and functional diversity. *National Science Review*, 2023, 10:nwac240(1-18).

[15] S. Sahoo, N. Deka, R. Panday, R. Boomishankar. Metal-free small molecule-based piezoelectric energy harvesters. *Chemical Communications*, 2024, 60:11655–11672.

[16] N. Deka, Sahoo, A. S. Goswami, J. K. Zaręba, R. Boomishankar. Homochirality-Induced Piezoelectricity in a Single-Component Molecular System. *Crystal Growth & Design*, 2024, 24:6763–6770.

[17] K Ding, H. Ye, C. Su, Y. A. Xiong, G. Du, Y. M. You, Z. X. Zhang, S. Dong, Y. Zhang, D. W. Fu. Superior ferroelectricity and nonlinear optical response in a hybrid germanium iodide hexagonal perovskite. *Nature Communications*, 2023, 14:2863(1-8).

[18] Aleksandrova, M.; Tudzharska, L.; Nedelchev, K.; Kralov, I. Hybrid Organic/Inorganic Piezoelectric Device for Energy Harvesting and Sensing Applications. *Coatings*, 2023, 13(2):464.

[19] Gincy Marina Mathew, Anoop Puthiyamadam, Keerthi Sasikumar, Selim Ashoor, Rajeev K. Sukumaran. Biological treatment of prawn shell wastes for valorization and waste management. *Bioresource Technology Reports*, 2021, 15: 100788.

[20] R. Muzzarelli, C. Jeuniaux, G. W. Gooday, Chitin in nature and technology, Plenum Publishing Corporation, New York, 1986.

[21] K. S. Mohammed, A. A. Nassani, S. A. Sarkodie. Assessing the effect of the aquaculture industry, renewable energy, blue R&D, and maritime transport on GHG emissions in Ireland and Norway. *Aquaculture*, 2024, 586: 740769.

[22] G. Caruso, R. Floris, C. Serangeli, and L. Di Paola, Fishery Wastes as a Yet Undiscovered Treasure from the Sea: Biomolecules Sources, Extraction Methods and Valorization. *Marine Drugs*, 2020, 18:622(1-30).

[23] K.V. Harish Prashanth, R.N. Tharanathan, Chitin/chitosan: modifications and their unlimited application potential-an overview. *Trends in Food Science & Technology*, 2007, 18:117-131.

[24] N. Vijayakumar, A. Velumani Sanjay, K. A. Al-Ghanim, M. Nicoletti, G. Baskar, Ranvijay Kumar, M. Govindarajan, Development of Biodegradable Bioplastics with Sericin and Gelatin from Silk Cocoons and Fish Waste. *Toxics*, 2024, 12:453.

[25] M. Asgher, S. A. Qamar, M. Bilal, H. M. Iqbal. Bio-based active food packaging materials: Sustainable alternative to conventional petrochemical-based packaging materials. *Food Research International*, 2020, 137:109625.

[26] G. A. F. Roberts. Thirty Years of Progress in Chitin and Chitosan. *Progress on chemistry and application of chitin*, 2008, 8(13):7-15.

[27] R. Gao, Q. Yu, Y. Shen, Q. Chul, C. Ge, S. Fen, M. Yang, L. Yuan, D. J. McClements, Q. Sun. Production, bioactive properties, and potential applications of fish protein hydrolysates: Developments and challenges. *Trends in Food Science & Technology*, 2021, 110: 687-699.

2025, by the Authors. The articles published from this journal are distributed to the public under “**Creative Commons Attribution License**” (<http://creativecommons.org/licenses/by/3.0/>). Therefore, upon proper citation of the original work, all the articles can be used without any restriction or can be distributed in any medium in any form.

#### Publication History

Received	25.08.2025
Revised	25.09.2025
Accepted	30.09.2025
Online	30.10.2025